geotechnics

MDPI

Article

Effect of Sample Preparation on Saturated and Unsaturated Shear Strength of Cohesionless Soils

Ilyas Akram and Shahid Azam *

Environmental Systems Engineering, Faculty of Engineering Applied Science, University of Regina, 3737 Wascana Parkway, Regina, SK S4S 0A2, Canada
* Correspondence: shahid.azam@uregina.ca

Abstract: The geotechnical behavior of cohesionless soils is governed by field conditions. Such soils exist in two distinct forms, namely: disintegrated, such as fresh sediments under no overburden and/or no suction, and intact, such as old deposits with overburden and/or suction. The main contribution of this research was the successful capture of field conditions in laboratory samples, and the determination of shear strength under saturated and dried states. Results indicated that disintegrated samples possess identical soil behavior under both saturation states. Shear stiffness and peak shear increased with increasing normal stress, and no clear failure peaks were observed, similar to loose soils. Both samples showed an initial contraction followed by dilation at low normal stresses and mostly contraction at high normal stresses. Apparent cohesion was non-existent, and the friction angle measured 44.5° in the saturated state and 48° in the dried state. The intact sample exhibited behavior similar to the disintegrated sample when saturated. Under the dried state, clear failure peaks followed by residual shear were observed, similar to dense soils. Soil response was primarily dilative at low normal stresses and largely contractive under high normal stresses. Apparent cohesion was zero, and friction angle was 42° in the saturated state and changed to 91 kPa and 36°, respectively, in the dried state. Finally, structural cohesion increased with normal stress, and the friction angle due to suction was between 0.05° and 0.02°.

Keywords: cohesionless soils; sample preparation; laboratory characterization; shear strength

Citation: Akram, I.; Azam, S. Effect of Sample Preparation on Saturated and Unsaturated Shear Strength of Cohesionless Soils. *Geotechnics* **2023**, *3*, 212–223. https://doi.org/10.3390/geotechnics3020013

Academic Editor: Abbas Taheri

Received: 10 March 2023
Revised: 4 April 2023
Accepted: 13 April 2023
Published: 16 April 2023

1. Introduction

The Canadian Prairies possess cohesionless soil deposits with extensive variability derived from physical weathering due to the wind (aeolian), water (alluvial or outside river boundaries and fluvial or inside river boundaries, and ice (glacial advances and retreats) [1]. Generally, such evolving processes cause surface sediments to occur in two conditions, namely: (i) disintegrated due to the absence of soil suction $(u_a - u_w)$, such as fresh deposits of unsorted glacio-fluvial pediments [2,3] or non-stratified aeolian loess [4,5] and (ii) intact due to the presence of soil suction, such as older alluvial deposits of stratified silt [6] or stratified loess and loess plateaus [7,8]; normal stress $(\sigma - u_a)$ is present in both cases. Given that the shear strength of cohesionless soils is governed by suction when unsaturated and by friction when saturated [9], it is critical to understand the engineering behavior of such soils under distinct field conditions.

The presence or absence of suction in cohesionless soils is related to post-depositional processes of cyclic saturation–desaturation [10]. The downward movement of a wetting front due to precipitation saturates the soil profile through infiltration, and the reverse process of exfiltration desaturates the same in the opposite direction [11]. During drying, water is gradually removed to increase soil suction at the air–water interface within the soil pores [12]. The thin water film around soil particles pulls the particles together to act as interparticle bonding [13]. This phenomenon of suction development forms intact cohesionless soils [2,14]. During wetting, water gradually displaces the pore air, thereby

reducing the negative pore pressure at the air–water interface to reduce interparticle bonding [15,16]. Clearly, interparticle bonding of suction is inversely proportional to the degree of saturation [17].

Figure 1 shows the conceptual relationship of shear stress with respect to stress state variables: normal stress is derived from overburden and governs soil density [18], whereas soil suction is derived from the atmosphere and governs soil saturation [19]. Under a given soil suction (Figure 1a), a linearly increasing relationship exists between shear stress and normal stress [20,21]. When soil suction is zero (saturated conditions), line A joins the ordinate at zero, indicating soil possesses no cohesion, and the slope pertains to the friction angle (φ'). When soil suction is more than zero (unsaturated condition), the intercept of line B denotes a higher value, which is known as apparent cohesion due to soil suction (c_ψ) [22,23]. Under a given normal stress (Figure 1b), a linearly increasing relationship exists between shear stress and soil suction. When normal stress is zero (surface soil), line C starts from zero because densification is non-existent [24], and the slope of line C denotes the friction angle due to suction (φ^b) [25]. When normal stress is more than zero (soil with overburden), line D starts from a higher intercept due to structural cohesion (c_{σ_n}) derived from compression [26,27], while φ^b mainly remains unchanged [9].

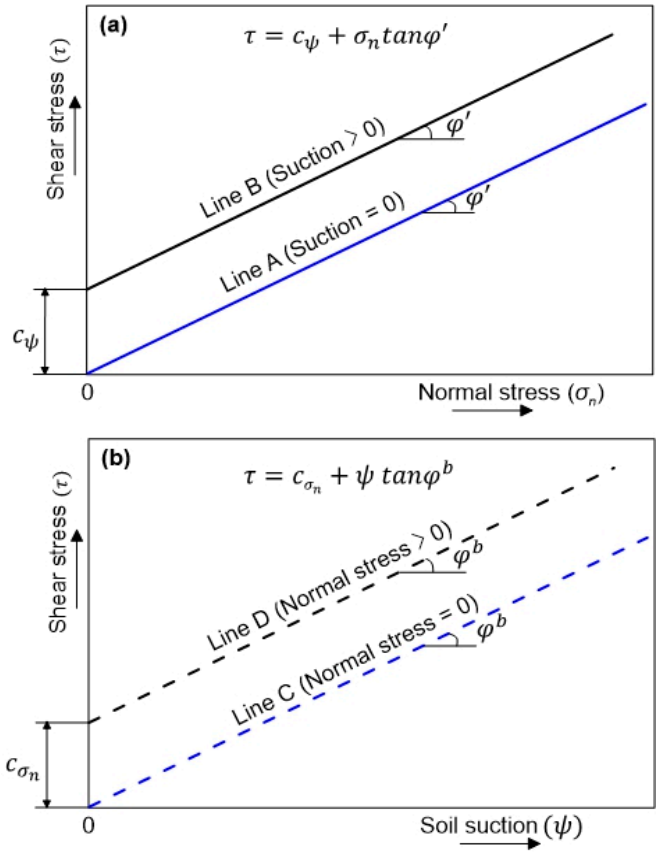

Figure 1. Conceptual shear stress variation of cohesionless soils with respect to independent state variables: (**a**) normal stress, (**b**) soil suction.

Table 1 summarizes the various methods for field retrieval and laboratory preparation of cohesionless samples. Among the field methods, sample disturbance is inevitable when using tube/piston samplers (above water table) or Bishop's samplers (below water table). Likewise, the use of soil impregnation or ground freezing techniques to minimize sample disturbance is difficult to execute and may be time-consuming and uneconomical within a project. Finally, block sampling is suitable for retrieving an undisturbed sample only when there is some binding within the soil particles. Among the laboratory preparation methods, wind and water deposition can be simulated using Air Pluviation (AP), Moist

Tamping (MT), Dry Deposition (DD), and Dry Tamping (DT). However, these methods have limitations in achieving high initial densities and sample uniformity. Likewise, the Water Sedimentation (WS) and Slurry Deposition (SD) are limited to saturated conditions only. Further, sample reconstitution and modified moist tamping methods mimicking intact in situ conditions are not suitable for cohesionless soils. This is because these methods do not represent cyclic saturation–desaturation of surface sediments. Although the DT is suitable for preparing disintegrated samples, a new laboratory sampling method is required to mimic the in situ intact samples in a desiccated state.

Table 1. Summary of sampling methods for cohesionless soils.

Methods and References	Purpose and Description	Limitations
Field Retrieval *Block sampling* [28–30]	To extrude undisturbed test samples from carefully trimmed and preserved in situ soil blocks.	Only applicable to soils possessing interparticle bonding through cementation and/or suction.
Tube sampling [31–37]	To retrieve samples at any depth using open tube (above water), Bishop's tube (below water), and sealed from sides using gel push samplers.	Sample size depends on tube diameter. Likewise, disturbance during drilling, retrieval, and extrusion.
Soil impregnation [38–40]	To minimize disturbance, heated gel is injected before retrieving samples using conventional drilling methods.	Complex field execution and sophisticated instruments needed to flush the impregnated solution before testing.
Soil freezing [41–44]	To stabilize the soil using liquid nitrogen prior to obtain samples through block or tube samplers.	Time-consuming, high operational cost, and special sample holders for storage and shipping.
Laboratory Preparation *Air pluviation (AP)* [45–48]	To mimic wind deposition process, soil is pluviated through a funnel by varying height and pluviation rate to control initial density.	Particle segregation. Also, non-uniformity increases with fine content due to lower falling velocities within a fixed drop height.
Moist tamping (MT) [49–52]	To replicate sediment deposition in water by mixing soil with in situ water content and tamping in layers.	Non-homogeneous ($\pm$10%) density in the sample due to variable compaction of soil layers.
Dry deposition (DD) [53–55]	To simulate surface deposition at low densities, dried soil is dropped from zero height by slowly raising the funnel.	Mostly suitable for cohesionless soils. Also, repeatability is difficult to maintain.
Dry tamping (DT) [56–58]	To mimic surface sediments subjected to in situ loading by tamping the top of samples prepared by *DD*.	Susceptible to particle crushing and difficult to achieve higher initial densities.
Water sedimentation (WS) [59–61]	To simulate the deposition of sediments in water bodies by placing the soil through a water-filled mold.	Only suitable for preparing saturated samples at low initial densities.
Slurry deposition (SD) [62–65]	To prepare uniform samples imitating in situ fabric by placing soil water mix in a container.	Applicable for saturated laboratory testing only.
Sample reconstitution [66–68]	To replicate undisturbed in situ soil samples by consolidating slurry prepared at 1.5 times the liquid limit.	Not suitable for cohesionless soils.
Modified moist tamping [57]	To mimic the unsaturated intact conditions by mixing soil with in situ water content followed by oven drying.	Does not replicate the cyclic saturation–desaturation of the cohesionless soils.

The main objective of this paper was to investigate the effect of sample preparation on the shear strength of cohesionless soils under distinct field conditions. Two types of samples were prepared [1]: disintegrated (*D*) and intact (*I*), such that each sample was tested under saturated and dried conditions. The direct shear test was employed due to its simple operation and the ability to easily test both sample types [69].

2. Research Methodology

Soil samples were collected from a typical fluvial deposit near Avonlea (latitude 50.0367 and longitude 105.0667), Saskatchewan, Canada. The up to 2 m thick deposit has a gentle slope of about 3° with the horizontal and contains cohesionless soils along the valley of a flow channel. The fresh surface sediment was found to have a water content (w) of 4% and a dry unit weight (γ_d) of 11 kN/m^3 [3]. Under desiccated conditions, the underlying deposit at 1 m depth was found to have a w of 2% and a γ_d of 14 kN/m^3. The suction value under such conditions was reported to be 10^5 kPa [1]. The soil was classified as silty sand (SM) with 36% material finer than 0.075 mm and moderate consistency (liquid limit of 27% and plastic limit of 23%), as reported by [70].

A pneumatically controlled direct shear apparatus was used to conduct the testing (Figure 2). The shear box assembly (containing the samples between two porous stones) was mounted on the apparatus and clamped. The displacements were determined by linear strain conversion transducers (HM-2310.10 for horizontal and HM-2310.04 for vertical measurement). Likewise, the shear stress was measured by an S-type transducer (HM-2300.020). The measured data were automatically recorded using a data acquisition system and transferred to a computer. The net normal stress of 25, 50, 125, and 300 kPa was applied pneumatically. Dried samples were allowed to equilibrate under each net normal stress for 24 h before shearing. In contrast, samples were inundated with water for 24 h after compression under a given net normal stress and subsequently sheared. A shearing rate of 0.05 mm/min was selected to preclude pore pressure build-up during shearing [71]. The tests were terminated after achieving 10 mm horizontal displacement (10% strain), samples were removed from the direct shear box, and the water content was measured for the saturated conditions. The shear strength at saturated and dried state was calculated by using the following two equations, respectively:

$$\tau = c_\psi + \sigma_n \, tan\varphi' \tag{1}$$

$$\tau = c_{\sigma_n} + \psi \, tan\varphi^b \tag{2}$$

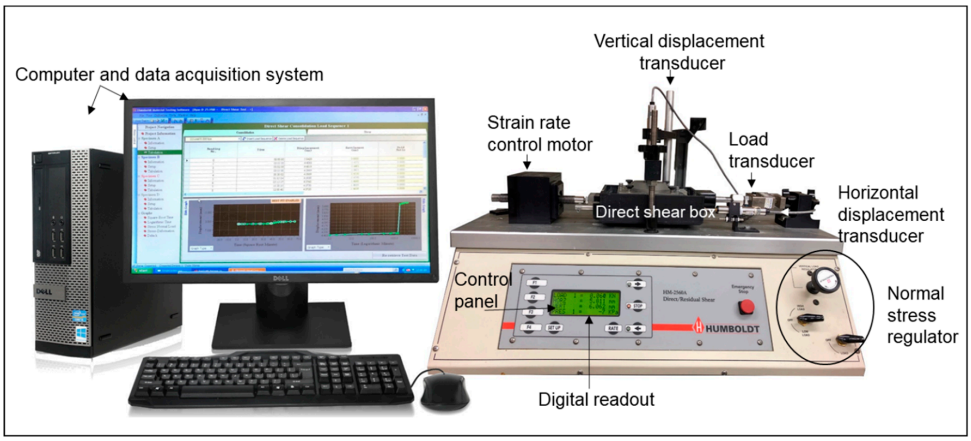

Figure 2. Experimental setup for the direct shear testing.

Figure 3 shows the different stages of *Sample D* during shear testing. Based on Cresswell et al. [72], a known amount of soil mass at 4% water content was poured into a direct shear ring (101.6 mm diameter and 26.8 mm height) and gently tamped with a wax rammer (50 mm diameter and 10 mm thickness) to obtain the desired density (11 kN/m^3) while avoiding particle crushing. The sample was prepared in the direct shear ring that provided lateral confinement (Figure 3a) and subsequently mounted on the direct shear machine (Figure 3b). Post-failure, the saturated sample (Figure 3c) showed a distinct failure plane, whereas the dried sample (Figure 3d) disintegrated due to the removal of lateral

confinement. It is pertinent to mention that the investigated soil changes color from light grey (Figure 3a) to dark grey (Figure 3c) with the addition of water [70].

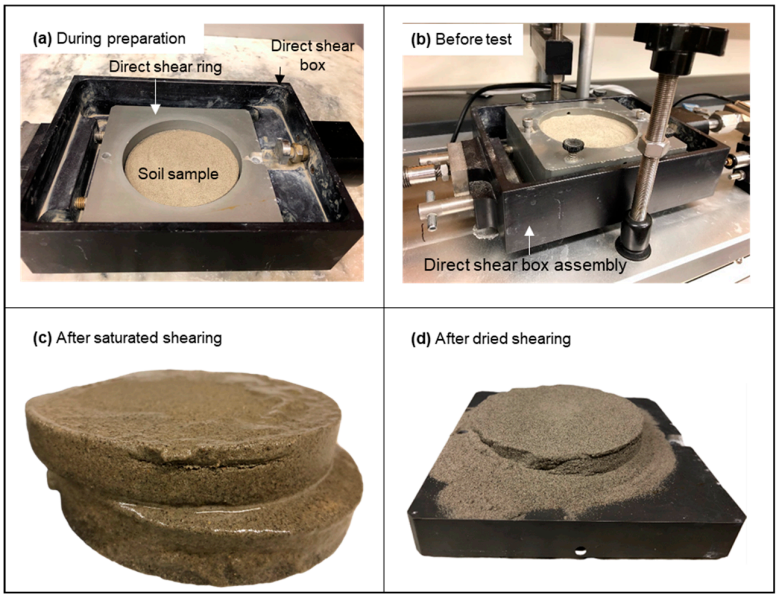

Figure 3. Sample *D* at various test stages during shear testing.

Figure 4 shows the different phases of *Sample I* during shear testing. As before, a known amount of soil mass at 2% water content was poured into the direct shear ring to obtain a density of 14 kN/m^3. Next, the sample was saturated by placing it in a water bath for 24 h and desaturation in a convection oven for 24 h. Unlike *Sample D*, this sample was prepared in the lower half of the direct shear ring (Figure 4a) because it was capable of standing without lateral support. The sample was mounted on the direct shear machine (Figure 4b). Post-failure, both the saturated (Figure 4c) and the dried (Figure 4d) samples exhibited distinct failure planes due to interparticle friction and suction bonding, respectively. The sample exhibited a color change (Figure 4c), as explained above.

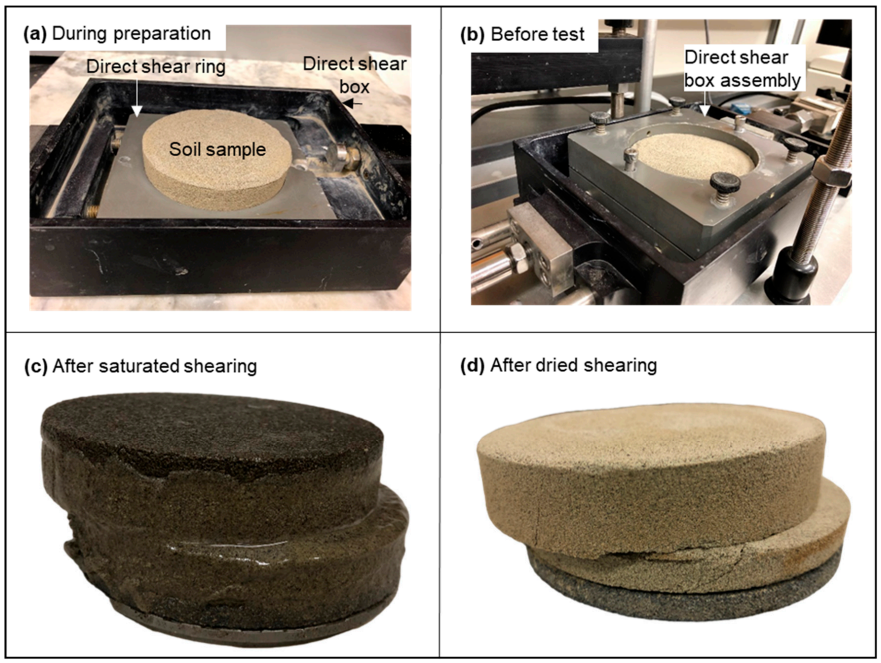

Figure 4. Sample *I* at various test stages during shear testing.

3. Results and Discussion

Figure 5 gives the test results for *Sample D*. Soil response is nearly identical under both saturated and dried conditions because of the absence of soil suction to provide interparticle bonding. From the shear stress versus horizontal displacement curves, the initial slope (shear stiffness) and the peak shear stress increased with increasing normal stress. This is due to densification that restricts the sliding of the soil particles along the shear plane [19,73]. Furthermore, both sample types exhibited a failure mode with no clear peaks under the given dry unit weight of 11 kN/m^3. This is a characteristic of loose cohesionless soils [74]. The slightly lower values of peak shear stress under the saturated state are attributed to particle lubrication that reduced interparticle bonding [75]. From the vertical displacement versus horizontal displacement curves, both sample types at low normal stresses of up to 50 kPa showed an initial contraction (moving of smaller particles in the void spaces between bigger particles) followed by dilation (insufficient space for soil particles to achieve a closer configuration) [24,76]. This wavy trend was found to obtain subdued high normal stresses where both sample types primarily showed a contractive behavior because of continuous particle rearrangement due to densification. Furthermore, this contractive behavior is independent of the soil type and degree of saturation [24,77].

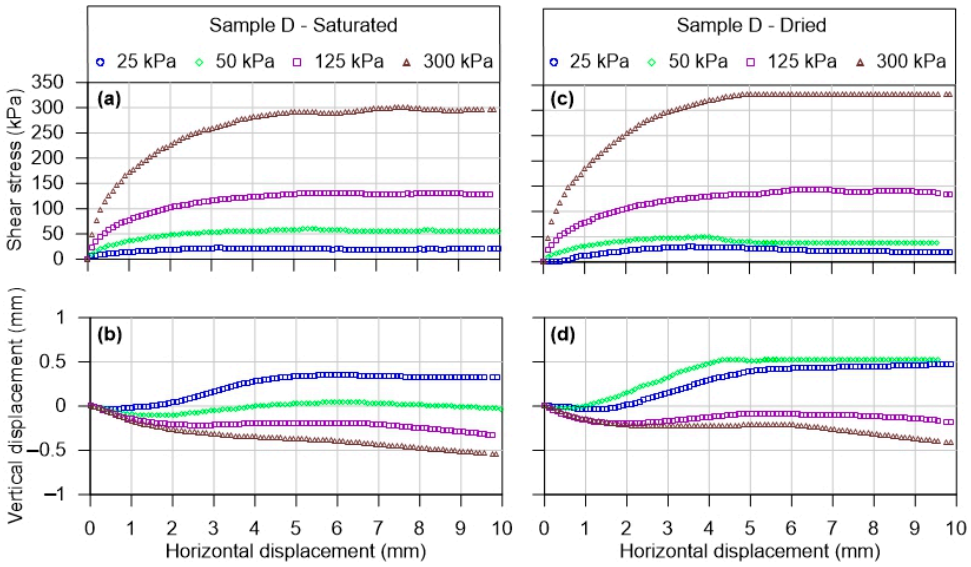

Figure 5. Test results for *Sample D*.

Figure 6 shows test results for *Sample I*. Soil behavior under saturated conditions was very similar to the previous sample. Due to the above-mentioned mechanisms, the shear stress versus horizontal displacement curve did not exhibit a clear peak at failure, and shear resistance increased with increasing normal stress. Likewise, the vertical displacement versus horizontal displacement curves showed contraction followed by dilation at a low normal stress of up to 50 kPa and primarily contraction at higher normal stress. Under dry conditions, where the initial data scatter is omitted, *Sample I* shows clear peak shear values such that the initial slopes remained nearly the same despite increasing normal stress. Thereafter, the samples showed residual shear similar to dense cohesionless soils. This trend is similar to elastoplastic softening behavior, where dense samples exhibit an initial linear portion followed by a peak at failure and then by residual values [78,79]. This behavior is attributed to the effect of soil suction that held the soil intact [80,81]. When compared with the saturated sample, soil behavior at low normal stresses of up to 50 kPa was primarily dilative because interparticle bonding due to suction precluded particle rearrangement. In contrast, soil behavior was found to be mostly contractive under high normal stresses because these stresses overcame the effect of suction and resulted in

continuous particle rearrangement due to densification. Again, this contractive behavior is independent of the soil type and degree of saturation [24,77].

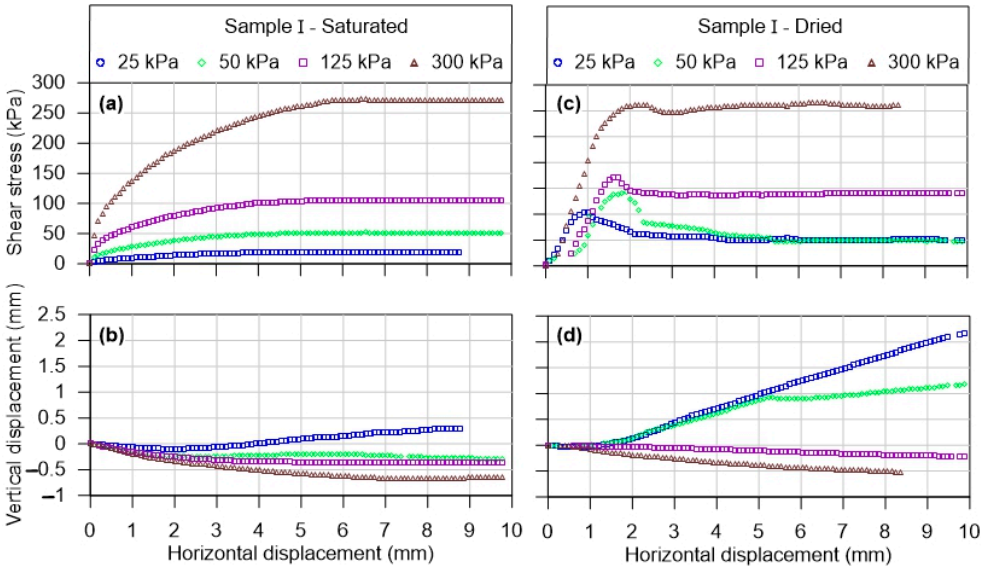

Figure 6. Test results for *Sample I*.

Under saturated states, the stress–strain behavior was identical irrespective of the sample type, although *Sample I* showed subdued initial dilation at a low normal stress of up to 50 kPa due to its relatively high initial γ_d of 14 kN/m^3. Under dried states, *Sample I* showed higher shear stress values and clear peaks at failure, whereas *Sample D* gave lower shear stress values (except at 300 kPa normal stress) and vague peaks at failure. Similarly, *Sample I* exhibited pronounced dilation up to 50 kPa normal stress when compared with *Sample D*. As mentioned before, these differences are attributed to the presence of interparticle bonding and the higher initial γ_d of *Sample I*.

Figure 7 and Table 2 show the shear strength parameters of the investigated soil under saturated and dried states. The peak shear stress versus normal stress data (Figure 7a) indicates the absence of apparent cohesion (c_ψ = 0) when the soil was either saturated and/or disintegrated. In contrast, c_ψ was found to be 91 kPa for *Sample I* (dried), as derived from interparticle bonding of suction [82]. The friction angle for *Sample D* was found to be 44.5° for the saturated state because of increased lubrication. This value increased to 48° for the dried state. These values are higher than the angle of repose (measured under no stress) primarily due to enhanced interlocking between soil particles under applied normal stresses [83]. An opposite trend was observed for *Sample I, in* which φ' decreased from 42° for the saturated state to 36° for the dried state because interparticle bonding due to suction reduced frictional resistance between particles [84,85]. Furthermore, the small variation in φ' (42° to 44.5°) under saturated conditions indicates that the effect of sample preparation is largely diminished due to saturation and that the discrepancy in measured values is attributed to experimental errors [61]. In contrast, the large variation in φ' (48° to 36°) under a dried state must be attributed to the effect of soil suction that is non-existent in *Sample D* but is dominant in *Sample I*. As mentioned earlier, interparticle bonding due to suction reduces frictional resistance between particles. For *Sample I*, which possesses suction, the lower φ' = 36° is compensated by c_ψ = 91 kPa, thereby increasing the shear strength of the soil at a given normal stress, as calculated by Equation (1).

Figure 7b shows the relationship between peak shear stress and soil suction. Both the saturated samples and the dried *Sample D* were plotted at an arbitrary suction of 1 kPa, which is lower than the air entry value (AEV) (8 kPa) of the investigated soil [70]. The dried *Sample I* was plotted at 10^5 kPa suction corresponding to the desiccated state. The line joining the two states (saturated and dried) of *Sample I* was used to determine the values

of c_{σ_n} and φ^b. At the ordinate, the c_{σ_n} values increased by 8 kPa (from 22 kPa to 30 kPa) at 25 kPa normal stress and by up to 62 kPa (from 270 kPa to 332 kPa) at 300 kPa normal stress. This increase in c_{σ_n} is attributed to increased particle packing under increasing normal stress [86]. Furthermore, φ^b was found to be between 0.02° and 0.05° based on the straight-line estimation. These values pertain to the dried state only and should not be taken as constant through the entire suction range. Generally, φ^b reduces non-linearly with increasing soil suction [87] and diminishes the residual suction range [9,85].

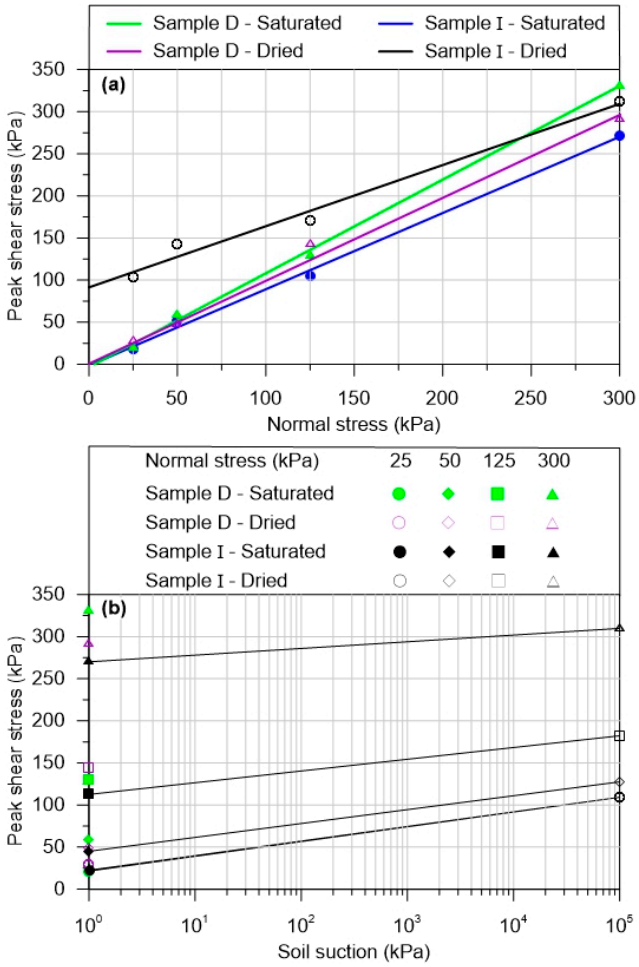

Figure 7. Observed shear stress variation of the investigated cohesionless soil with respect to independent state variables: (**a**) normal stress, (**b**) soil suction.

Table 2. Summary of shear strength parameters.

Sample Type	Sample Condition	Normal Stress (kPa)	Soil Suction (kPa)	c_ψ (kPa)	c_{σ_n} (kPa)	φ'	φ^b
Sample D	Saturated	-	-	0	-	44.5°	
	Dried	-	-	0	-	48.0°	
Sample I	Saturated	-	-	0	-	42.0°	
	Dried	-	10^5	91	-	36.1°	
		25	-	-	23	-	0.05°
		50	-	-	45	-	0.05°
		125	-	-	112	-	0.04°
		300	-	-	270	-	0.02°

4. Summary and Conclusions

Knowledge of field setting is critical for understanding the behavior of cohesionless soils. The main contribution of this research includes the following: (i) successful capture of in situ conditions by developing a laboratory sample preparation procedure and (ii) development of a clear understanding of the shear strength behavior under saturated and dried states. The findings of this research are summarized as follows:

- The disintegrated samples showed identical soil responses under saturated and dried conditions. The initial slope (shear stiffness) and the peak shear stress increased with increasing normal stress, and no clear peaks were observed at the failure, similar to loose soils. Both samples showed an initial contraction followed by dilation at low normal stresses and mostly a contractive behavior at high normal stresses. Furthermore, apparent cohesion was non-existent and φ' was found to be 44.5° in the saturated state and 48° in the dried state.
- The intact sample exhibited behavior similar to the disintegrated sample in the saturated state. Under the dried state, the sample showed clear peaks at failure followed by residual shear similar to dense soils or elastoplastic softening behavior. Soil behavior was dilative at low normal stresses and largely contractive under high normal stresses. Likewise, apparent cohesion was zero, and φ' was 42° in the saturated state and changed to 91 kPa and 36°, respectively, in the dried state. For the latter state, structural cohesion increased with normal stress, and φ^b was found to be between 0.05° and 0.02°.

Author Contributions: Investigation, I.A.; data curation and analysis, I.A.; conceptualization, S.A.; supervision, S.A.; writing—original draft, I.A.; writing—review and editing, S.A. All authors have read and agreed to the published version of the manuscript.

Funding: Natural Science and Engineering Research Council of Canada and SaskEnergy Inc. through a collaborative research and development grant.

Data Availability Statement: The authors can provide access to test data upon request.

Acknowledgments: The authors thank the University of Regina for providing laboratory testing facilities.

Conflicts of Interest: The authors declare there are no conflict of interest.

References

1. Akram, I.; Azam, S. Determination of Collapse and Consolidation Behavior of Cohesionless Soils. *Bull. Eng. Geol. Environ.* **2022**, *81*, 458. [CrossRef]
2. Earle, S. *Physical Geology*; Open Text; McGraw Hill: Vancouver, BC, Canada, 2015.
3. Azam, S.; Khan, F. Geohydrological Properties of Selected Badland Sediments in Saskatchewan, Canada. *Bull. Eng. Geol. Environ.* **2014**, *73*, 389–399. [CrossRef]
4. Catt, J.A. Loess-Its Formation, Transport and Economic Significance. In *Physical and Chemical Weathering in Geochemical Cycles*; Kluwer Academic Publishers: Boston, MA, USA, 1988.
5. Slaymaker, O.; Catto, N. *Landscapes and Landforms of Eastern Canada*; Springer Nature: Berlin, Germany, 2020.
6. Knipperts, P.; Stuut, J.B.W. *Mineral Dust-A Key Player in the Earth System*; Springer: Berlin, Germany, 2014.
7. Li, Y.; Shi, W.; Aydin, A.; Beroya-Eitner, M.A.; Gao, G. Loess Genesis and Worldwide Distribution. *Earth Sci. Rev.* **2020**, *201*, 102947. [CrossRef]
8. Xu, J.; Wei, W.; Bao, H.; Zhang, K.; Lan, H.; Yan, C.; Wu, F. Study on Shear Strength Characteristics of Loess Dam Materials under Saturated Conditions. *Environ. Earth Sci.* **2020**, *79*, 346. [CrossRef]
9. Huat, B.K.; Ali, F.H.; Hashim, S. Modified Shear Box Test Apparatus for Measuring Shear Strength of Unsaturated Residual Soil. *Am. J. Appl. Sci.* **2005**, *2*, 1283–1289. [CrossRef]
10. Houston, S.L.; Houston, W.N.; Zapata, C.E.; Lawrence, C. Geotechnical Engineering Practice for Collapsible Soils. In *Unsaturated Soil Concepts and their Application in Geotechnical Practice*; Springer: Berlin, Germany, 2001.
11. Azam, S.; Ito, M. Coupled Soil-Atmosphere Modeling for Expansive Regina Clay. *J. Environ. Inform.* **2012**, *19*, 20–29. [CrossRef]
12. Ng, C.W.W.; Menzies, B. *Advanced Unsaturated Soil Mechanics and Engineering*; Taylor and Francis: New York, NY, USA, 2007.
13. Karube, D.; Kawai, K. The Role of Pore Water in the Mechanical Behavior of Unsaturated Soils. *Geotech. Geol. Eng.* **2001**, *19*, 211–241. [CrossRef]

14. Komolvilas, V.; Kikumoto, M.; Kyokawa, H. Mechanism of Wetting–Induced Deformation and Failure of Unsaturated Soils. *Int. J. Numer. Anal. Methods Geomech.* **2022**, *46*, 1064–1092. [CrossRef]
15. Li, P.; Vanapalli, S.K.; Li, T. Review of Collapse Triggering Mechanism of Collapsible Soils Due to Wetting. *J. Rock Mech. Geotech. Eng.* **2016**, *8*, 256–274. [CrossRef]
16. Ravindran, S.; Gratchev, I. Effect of Water Content on Apparent Cohesion of Soils from Landslide Sites. *Geotechnics* **2022**, *2*, 385–394. [CrossRef]
17. Gallipoli, D.; Gens, A.; Sharma, R.; Vaunat, J. An Elasto-Plastic Model for Unsaturated Soil Incorporating the Effects of Suction and Degree of Saturation on Mechanical Behaviour. *Géotechnique* **2003**, *53*, 123–135. [CrossRef]
18. Sun, D.; Sheng, D.; Xu, Y. Collapse Behaviour of Unsaturated Compacted Soil with Different Initial Densities. *Can. Geotech. J.* **2007**, *44*, 673–686. [CrossRef]
19. Lu, N.; Likos, W.J. *Unsaturated Soil Mechanics*; John Wiley and Sons Inc.: New York, NY, USA, 2004.
20. Hamidi, A.; Azini, E.; Masoudi, B. Impact of Gradation on the Shear Strength-Dilation Behavior of Well Graded Sand-Gravel Mixtures. *Sci. Iran.* **2012**, *19*, 393–402. [CrossRef]
21. Sun, S.; Xu, H. Determining the Shear Strength of Unsaturated Silt. In *Experimental Unsaturated Soil Mechanics*; Springer: Berlin, Germany, 2007; pp. 195–206.
22. Li, Z.W.; Yang, X.L. Active Earth Pressure from Unsaturated Soils with Different Water Levels. *Int. J. Geomech.* **2019**, *19*, 1–10. [CrossRef]
23. Zhang, L.L.; Fredlund, D.G.; Fredlund, M.D.; Wilson, G.W. Modeling the Unsaturated Soil Zone in Slope Stability Analysis. *Can. Geotech. J.* **2014**, *51*, 1384–1398. [CrossRef]
24. Gallage, C.; Uchimura, T. Direct Shear Testing on Unsaturated Silty Soils to Investigate the Effects of Drying and Wetting on Shear Strength Parameters at Low Suction. *J. Geotech. Geoenviron. Eng.* **2016**, *142*, 1–9. [CrossRef]
25. Fredlund, D.G.; Rahardjo, H.; Fredlund, M.D. *Unsaturated Soil Mechanics in Engineering Practice*; John Wiley and Sons Inc.: New York, NY, USA, 2012.
26. Feuerharmel, C.; Pereira, A.; Gehling, W.Y.Y.; Bica, A.V.D. Determination of the Shear Strength Parameters of Two Unsaturated Colluvium Soils Using the Direct Shear Test. In Proceedings of the Unsaturated Soils (UNSAT), Beijing, China, 27 August 2006; pp. 1181–1190.
27. Gao, Y.; Sun, D.; Zhou, A.; Li, J. Predicting Shear Strength of Unsaturated Soils over Wide Suction Range. *Int. J. Geomech.* **2020**, *20*, 1–11. [CrossRef]
28. Fonseca, J.; O'sullivan, C.; Coop, M.R.; Lee, P.D. Quantifying the Evolution of Soil Fabric during Shearing Using Directional Parameters. *Géotechnique* **2013**, *63*, 487–499. [CrossRef]
29. Lim, G.T.; Pineda, J.; Boukpeti, N.; Carraro, J.A.H.; Fourie, A. Effects of Sampling Disturbance in Geotechnical Design. *Can. Geotech. J.* **2019**, *56*, 275–289. [CrossRef]
30. Sadeghi, H.; Kiani, M.; Sadeghi, M.; Jafarzadeh, F. Geotechnical Characterization and Collapsibility of a Natural Dispersive Loess. *Eng. Geol.* **2019**, *250*, 89–100. [CrossRef]
31. Andresen, A. The NGI 54-Mm Samplers for Undisturbed Sampling of Clays and Representative Sampling of Coarser Materials, State of the Art on Current Practice of Soil Sampling. In *Proceedings of the International Symposium of Soil Sampling*; Springer: Singapore; p. 1979.
32. Bishop, A.W. A New Sampling Tool for Use in Cohesionless Sands below Ground Water Level. *Geotechnique* **1948**, *1*, 125–136. [CrossRef]
33. Blaker, Ø.; DeGroot, D.J. Intact, Disturbed, and Reconstituted Undrained Shear Behavior of Low-Plasticity Natural Silt. *J. Geotech. Geoenviron. Eng.* **2020**, *146*, 1–14. [CrossRef]
34. Bray, J.D.; Sancio, R.B.; Durgunoglu, T.; Onalp, A.; Youd, T.L.; Stewart, J.P.; Seed, R.B.; Cetin, K.O.; Bol, E.; Baturay, M.B. Subsurface Characterization at Ground Failure Sites in Adapazari, Turkey. *J. Geotech. Geoenviron. Eng.* **2004**, *130*, 673–685. [CrossRef]
35. Long, M. Engineering Characterization of Estuarine Silts. *Q. J. Eng. Geol. Hydrogeol.* **2007**, *40*, 147–161. [CrossRef]
36. Mori, K.; Sakai, K. The GP Sampler: A New Innovation in Core Sampling. *Aust. Geomech. J.* **2016**, *51*, 131–166.
37. Quinteros, V.S.; Carraro, J.A.H. The Initial Fabric of Undisturbed and Reconstituted Fluvial Sand. *Geotechnique* **2021**, *73*, 1–15. [CrossRef]
38. Evans, T. Microscale Physical and Numerical Investigations of Shear Banding in Granular Soils. Ph.D. Thesis, Georgia Institute of Technology, Atlanta, GA, USA, 2005.
39. Schneider, H.R.; Chameau, J.L.; Leonards, G.A. Chemical Impregnation of Cohesionless Soils. *Geotech. Test. J.* **1989**, *12*, 201–210.
40. Sutterer, K.G.; Frost, J.D.; Chameau, J.L. Polymer Impregnation to Assist Undisturbed Sampling of Cohesionless Soils. *J. Geotech. Eng.* **1996**, *122*, 209–215. [CrossRef]
41. Blevins, R.L.; Aubertin, G.M.; Holowaychuk, N. A Technique for Obtaining Undisturbed Soil Samples by Freezing in Situ. *Soil Sci. Soc. Am. J.* **1968**, *32*, 741–742. [CrossRef]
42. Hofmann, B.A.; Sego, D.C.; Robertson, P.K. In Situ Ground Freezing to Obtain Undisturbed Samples of Loose Sand. *J. Geotech. Geoenviron. Eng.* **2000**, *126*, 979–989. [CrossRef]
43. Sego, D.C.; Robertson, P.K.; Sasitharan, S.; Kllpatrick, B.L.; Pillai, V.S. Ground Freezing and Sampling of Foundation Soils at Duncan Dam. *Can. Geotech. J.* **1994**, *31*, 939–950. [CrossRef]

44. Yoshimi, Y.; Hatanaka, M.; Oh-oka, H. Undisturbed Sampling of Saturated Sands by Freezing. *Soils Found.* **1978**, *18*, 59–73. [CrossRef]
45. Amini, F.; Chakravrty, A. Liquefaction Testing of Layered Sand-Gravel Composites. *Geotech. Test. J.* **2004**, *27*, 36–46.
46. Juneja, A.; Raghunandan, M.E. Effect of Sample Preparation on Strength of Sands. In Proceedings of the Indian Geotechnical Conference, Mumbai, India, 16 December 2010; pp. 327–330.
47. Sadrekarimi, A.; Olson, S.M. Effect of Sample-Preparation Method on Critical-State Behavior of Sands. *Geotech. Test. J.* **2012**, *35*, 548–562. [CrossRef]
48. Vaid, Y.P.; Negussey, D. Relative Density of Pluviated Sand Samples. *Soils Found.* **1984**, *24*, 101–105. [CrossRef]
49. Della, N.; Arab, A.; Belkhatir, M. Drained and Undrained Shear Strength of Silty Sand: Effect of the Reconstruction Methods and Other Parameters. *Geol. Croat.* **2011**, *64*, 163–171. [CrossRef]
50. Dijkstra, T.A.; Rogers, C.D.F.; Smalley, I.J.; Derbyshire, E. The Loess of North-Central China: Geotechnical Properties and Their Relation to Slope Stability. *Eng. Geol.* **1994**, *36*, 153–171. [CrossRef]
51. Frost, J.D.; Park, J.Y. A Critical Assessment of the Moist Tamping Technique. *Geotech. Test. J.* **2003**, *26*, 57–70.
52. Olson, S.M.; Stark, T.D.; Walton, W.H.; Castro, G. 1907 Static Liquefaction Flow Failure of the North Dike of Wachusett Dam. *J. Geotech. Geoenviron. Eng.* **2000**, *126*, 1184–1193. [CrossRef]
53. Bensoula, M.; Missoum, H.; Bendani, K. Critical Undrained Shear Strength of Sand-Silt Mixtures under Monotonic Loading. *Earth Sci. Res. J.* **2014**, *18*, 149–156. [CrossRef]
54. Sze, H.Y.; Yang, J. Failure Modes of Sand in Undrained Cyclic Loading: Impact of Sample Preparation. *J. Geotech. Geoenviron. Eng.* **2014**, *140*, 152–169. [CrossRef]
55. Zlatovic, S.; Ishihara, K. Normalized Behavior of Very Loose Non-Plastic Soils: Effects of Fabric. *Soils Found.* **1997**, *37*, 47–56. [CrossRef] [PubMed]
56. Ishihara, K. Liquefaction and Flow Failure during Earthquakes. *Geotechnique* **1993**, *43*, 351–451. [CrossRef]
57. Li, Y.; Yang, Y.; Yu, H.; Roberts, G. Effect of Sample Reconstitution Methods on the Behaviors of Granular Materials under Shearing. *J. Test. Eval.* **2018**, *46*, 1–23. [CrossRef]
58. Yang, Z.X.; Li, X.S.; Yang, J. Quantifying and Modelling Fabric Anisotropy of Granular Soils. *Géotechnique* **2008**, *58*, 237–248. [CrossRef]
59. Mulilis, J.P.; Seed, H.B.; Chan, C.K.; Mitchell, J.K.; Arulanandan, K. Effects of Sample Preparation on Sand Liquefaction. *J. Geotech. Eng. Division* **1977**, *103*, 91–108. [CrossRef]
60. Tatsuoka, F.; Ochi, K.; Fujii, S.; Okamoto, M. Cyclic Undrained Triaxial and Torsional Shear Strength of Sands for Different Sample Preparation Methods. *Soils Found.* **1986**, *26*, 23–41. [CrossRef]
61. Wanatowski, D.; Chu, J. Effect of Specimen Preparation Method on the Stress-Strain Behavior of Sand in Plane-Strain Compression Tests. *Geotech. Test. J.* **2008**, *31*, 1–14.
62. Krage, C.P.; Price, A.B.; Lukas, W.G.; DeJong, J.T. Slurry Deposition Method of Low-Plasticity Intermediate Soils for Laboratory Element Testing. *Geotech. Test. J.* **2019**, *43*, 1269–1285. [CrossRef]
63. Kuerbis, R.; Vaid, Y.P. Sand Sample Preparation-the Slurry Deposition Method. *Soils Found.* **1988**, *28*, 107–118. [CrossRef]
64. Yamamuro, J.A.; Wood, F.M. Effect of Depositional Method on the Undrained Behavior and Microstructure of Sand with Silt. *Soil Dyn. Earthq. Eng.* **2004**, *24*, 751–760. [CrossRef]
65. Yin, K.; Liu, J.; Vasilescu, A.R.; Di Filippo, E.; Othmani, K. A Procedure to Prepare Sand–Clay Mixture Samples for Soil–Structure Interface Direct Shear Tests. *Appl. Sci.* **2021**, *11*, 5337. [CrossRef]
66. Burland, J.B. On the Compressibility and Shear Strength of Natural Clays. *Géotechnique* **1990**, *40*, 329–378. [CrossRef]
67. Stephens, I.; Branch, A. *Testing Procedure for Estimating Fully Softened Shear Strengths of Soils Using Reconstituted Material*; Engineer Research and Development Center Vicksburg MS Geotechnical: Vicksburg, MS, USA, 2013.
68. Yin, J. Mechanical Behavior of Reconstituted Clay Samples Prepared by Large Diameter Oedometer. In *Civil Engineering and Urban Planning 2012*; American Society of Civil Engineers: Reston, VA, USA, 2012; pp. 362–368.
69. Beren, M.; Cobanoglu, I.; Çelik, S.B.; Ündül, O. Shear Rate Effect on Strength Characteristics of Sandy Soils. *Soil Mech. Found. Eng.* **2020**, *57*, 287. [CrossRef]
70. Akram, I.; Azam, S. Determination of Saturated-Unsaturated Flow through Silty Sand. *Geotech. Geol. Eng.* **2022**, *40*, 469–481. [CrossRef]
71. ASTM International. ASTM-D3080 Standard Test Method for Direct Shear Tests of Soils under Consolidated Drained Conditions. In *Annual Book of ASTM Standards*; ASTM International: West Conshohocken, PA, USA, 2011.
72. Cresswell, A.; Barton, M.E.; Brown, R. Determining the Maximum Density of Sands by Pluviation. *Geotech. Test. J.* **1999**, *22*, 324–328.
73. Budhu, M. *Soil Mechanics and Foundations*; John Wiley and Sons Inc.: New York, NY, USA, 2011.
74. Clayton, P.; Kam, W.Y.; Beer, A. Interaction of Geotechnical and Structural Engineering in the Seismic Assessment of Existing Buildings. In Proceedings of the Annual Conference NZSEE, Richmond, CA, USA, 21 March 2014.
75. Jafarzadeh, F.; Ahmadinezhad, A.; Sadeghi, H. Coupled Effects of Suction and Degree of Saturation on Large Strain Shear Modulus of Unsaturated Sands. In *Unsaturated Soils: Research & Applications*; CRC Press: Leiden, The Netherlands, 2020; pp. 1559–1564.
76. Høeg, K.; Dyvik, R.; Sandbækken, G. Strength of Undisturbed versus Reconstituted Silt and Silty Sand Specimens. *J. Geotech. Geoenviron. Eng.* **2000**, *126*, 606–617. [CrossRef]

77. Bro, A.D.; Stewart, J.P.; Pradel, D. Estimating Undrained Strength of Clays from Direct Shear Testing at Fast Displacement Rates. In Proceedings of the Geo-Congress 2013: Stability and Performance of Slopes and Embankments III, San Diego, CA, USA, 30 May 2013; pp. 106–119.
78. Song, A.; Pineda-Contrreras, A.R.; Medina-Cetina, Z. Modeling of Sand Triaxial Specimens under Compression:Introducing an Elasto-Plastic Finite Element Model to Capture the Impact of Specimens' Heterogeneity. *Minerals* **2023**, *13*, 498. [CrossRef]
79. Zhang, Y.; Wang, L.; Zi, G.; Zhang, Y. Mechanical Behavior of Coupled Elastoplastic Damage of Clastic Sandstone of Different Burial Depths. *Energies* **2020**, *13*, 1640. [CrossRef]
80. Guan, G.S.; Rahardjo, H.; Choon, L.E. Shear Strength Equations for Unsaturated Soil under Drying and Wetting. *J. Geotech. Geoenviron. Eng.* **2010**, *136*, 594–606. [CrossRef]
81. Hormdee, D.; Ochiai, H.; Yasufuku, N. Advanced Direct Shear Testing for Collapsible Soils with Water Content and Matric Suction Measurement. In *Site Characterization and Modeling*; American Society of Civil Engineers: Reston, VA, USA, 2005; pp. 1–10.
82. Vahedifard, F.; Leshchinsky, B.A.; Mortezaei, K.; Lu, N. Active Earth Pressures for Unsaturated Retaining Structures. *J. Geotech. Geoenviron. Eng.* **2015**, *141*, 1–10. [CrossRef]
83. Al-Hashemi, H.M.B.; Al-Amoudi, O.S.B. A Review on the Angle of Repose of Granular Materials. *Powder Technol.* **2018**, *330*, 397–417. [CrossRef]
84. Likos, W.J.; Wayllace, A.J.; Lu, N. Modified Direct Shear Apparatus for Unsaturated Sands at Low Suction and Stress. *Geotech. Test. J.* **2010**, *33*, 286–298.
85. Abd, I.A.; Fattah, M.Y.; Mekkiyah, H. Relationship between the Matric Suction and the Shear Strength in Unsaturated Soil. *Case Stud. Constr. Mater.* **2020**, *13*, e00441. [CrossRef]
86. Rivera-Hernandez, X.A.; Vahedifard, F.; Ellithy, G.S. Effect of Suction and Confining Pressure on Shear Strength and Dilatancy of Highly Compacted Silty Sand: Single-Stage versus Multistage Triaxial Testing. *Geotech. Test. J.* **2020**, *44*, 407–421. [CrossRef]
87. Chowdhury, R.H.; Azam, S. Unsaturated Shear Strength Properties of a Compacted Expansive Soil from Regina, Canada. *Innov. Infrastruct. Solut.* **2016**, *1*, 47. [CrossRef]